# Edge-Preserving Tomographic Reconstruction With Nonlocal Regularization

Daniel F. Yu and Jeffrey A. Fessler
4415 EECS Bldg., University of Michigan, Ann Arbor, MI 48109-2122
fyz@eecs.umich.edu

**Abstract**

*We propose a new objective function for the image reconstruction problem, where the image is comprised of piecewise smooth regions separated by sharp boundaries. We use alternating minimization to minimize our objective function. We use the level set technique to minimize with regard to the boudary. The advantage of this new approach is shown through the bias/variance analysis of a hot spot.*

## 1 Introduction

Tomographic image reconstruction using statistical methods can provide more accurate system modeling, statistical models, and physical constraints than the conventional filtered backprojection (FBP) method. But usually, this problem is ill posed and a roughness penalty must be imposed on the solution. To avoid smoothing of edges, which are important attributes of the image, various edge-preserving regularization schemes have been proposed. Most of these schemes rely on information from a *local* neighbourhood to determine the existence of edges, e.g., [1] and [2]. In this paper, we propose an objective function that incorporates *nonlocal* boundary information into regularization. We use an alternating minimization scheme that partly uses recent advances in level set techniques in the field of image segmentation [3] [4]. Teboul *et al* applied the level set approach to image restoration [5]; we extend their approach and apply it to image reconstruction. We also do some preliminary comparison of the bias/variance tradeoff of the proposed method with the nonquadratic penalized least-squares algorithm [6] [7] to show the advantage of using the new method.

## 2 Penalized Least-Squares Image Reconstruction for PET

We assume the system model,

$$Y = \mathbf{A}\lambda + n \tag{1}$$

where $n$ is measurement noise, $Y$ is the sinogram, $\lambda$ is the object we are interested in, and $\mathbf{A}$ is the system matrix. The goal is to estimate $\lambda$ from $Y$, but this is an ill-posed problem. A standard approach is to minimize the following objective function:

$$\Phi(\lambda) = \frac{1}{2}\|y - \mathbf{A}\lambda\|^2 + \beta R(\lambda)$$

$$R(\lambda) = \sum_j \sum_{k \in N_j} w_{jk}\psi(\lambda_j - \lambda_k), \tag{2}$$

where $\psi$ is a penalty function such as the Huber function which helps to preserve edges, and $N_j$ consists of the left and upper neighbors of pixel $j$. If $\psi$ is the Huber function, the objective function is convex, thus it can be minimized very efficiently using the coordinate descent algorithm [7]. However, the regularization in equation (2) is only local; there is no "global" structure in the regularization, so it is plausible that the regularization described in equation (2) is suboptimal. Therefore, we are investigating the use of active contour/level set to develop a more global approach, for objects that are piecewise smooth with piecewise smooth boundaries.

## 3 Image Segmentation Using Level Sets

Level set techniques were originally proposed by Osher and Sethian [8]. Malladi *et al* [9] proposed a front propagation/level set approach for image segmentation. In this paper, we use the new active contour paradigm proposed by Yezzi *et al* [4]. A key innovation in [4] is changing the ordinary Euclidean arc-length function along a curve $C = (x(p), y(p))^T$ with parameter $p$ from

$$ds = \|C_p\|dp = ({x_p}^2 + {y_p}^2)^{1/2}dp$$

to

$$ds_\phi = \phi_\lambda ds = \phi_\lambda({x_p}^2 + {y_p}^2)^{1/2}dp$$

where $\phi_\lambda(x, y)$ is a positive differentiable function. A new length function results:

$$L_{\phi_\lambda}(t) \triangleq \int_0^1 \left\| \frac{\partial C}{\partial p} \right\| \phi_\lambda dp \tag{3}$$

A contour can be evolved using level set techniques so that the new length function is minimized. If $\phi_\lambda$ is defined in such a way so that it is small where the local gradient of



0-8186-8821-1/98 $10.00 

the image $\lambda$ is large, and large where the local gradient is small, then the final contour comes to rest on the boundary of the shape. This method combines the advantage of both classical energy methods and the geometric curve evolution models. It is based on first principles and the flow is derived directly to minimize the energy of the contour.

## 4 A New Approach to Edge-Preserving Regularization

If the reconstructed image is to have unblurred boundaries, the pixel values must be "decoupled" across the edges, i.e., the $w_{jk}$'s in equation (2) must be set to zero at those places. We choose to formulate the problem in the discrete domain, and approximate the length functional defined in equation (3) with the following:

$$L_\phi = \sum_{(x,y)\in B} \phi_\lambda(x,y).$$

We propose the following objective function of the image $\lambda$ and the auxiliary variable $B$ (for boundary):

$$\begin{aligned}
\Phi(\lambda, B) &= \frac{1}{2}\|y - \mathbf{A}\lambda\|^2_{\mathbf{W}} + \beta R(\lambda, B) + \frac{\gamma}{n_B} S(\lambda, B) \\
R(\lambda, B) &= \sum_{(j,k)\in N} h(j,k,B)(\lambda_j - \lambda_k)^2 \\
S(\lambda, B) &= \sum_{(j,k)\in B} \phi_\lambda(j,k),
\end{aligned}$$

where

$$h(j,k,B) = \begin{cases} 0 & \text{if } (j,k)\in B \\ 1 & \text{otherwise,} \end{cases} \tag{4}$$

$B$ is the set of neighboring pixel pairs $(j,k)$ between which pixel values should be "decoupled" (*i.e.*, penalty on the difference set to 0), $N$ is the set of all neighboring pixel pairs $(j,k)$, $n_B$ is the number of pixel pairs belonging to $N$, and $\lambda$ is the discrete image. The first term $\frac{1}{2}\|y - \mathbf{A}\lambda\|^2_{\mathbf{W}}$ measures the "faithfulness" of the reconstructed image to the measured data. The second term $R(\lambda, B) = \sum_{(j,k)\in N} h(j,k,B)(\lambda_j - \lambda_k)^2$ penalizes the differences in pixel values between neighboring pixels, everywhere except on the boundary where the difference is not penalized at all (because $h$ is set to 0 at these locations). The third term $S(\lambda, B) = \sum_{(j,k)\in B} \phi_\lambda(j,k)$ is the penalty for the estimate of the boundary; it is minimized when all pixel pairs in $B$ are on the boundary.

We use alternating minimization to jointly minimize this objective function over the object $\lambda$ and boundary $B$. (Note that the boundary is not known in advance, but is determined iteratively as the image is reconstructed.) When $\lambda$ is fixed,

$$R(\lambda, B) = \sum_{(j,k)\in N} (\lambda_j - \lambda_k)^2 - \sum_{(j,k)\in B} (\lambda_j - \lambda_k)^2 \tag{5}$$

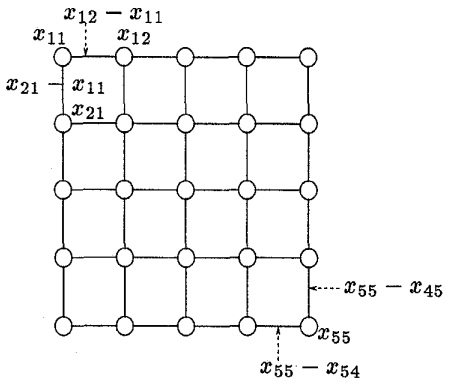


Figure 1: A circle denotes a pixel, while a line between 2 pixels denote the difference between pixel values.

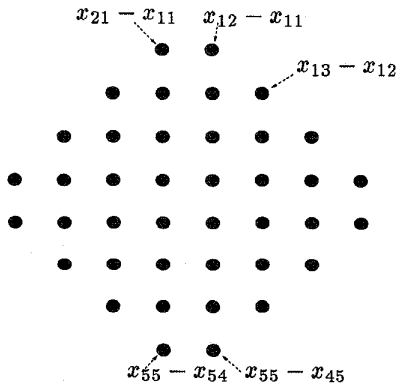


Figure 2: The lines are represented by black circles to show that the lines form an "image" by themselves.

The first term in equation (5) and $\frac{1}{2}\|y - \mathbf{A}\lambda\|^2_{\mathbf{W}}$ do not depend on $B$, thus they can be ignored. Then we have:

$$\Phi_\lambda(B) = -\beta \sum_{(j,k)\in B} (\lambda_j - \lambda_k)^2 + \frac{\gamma}{n_B} \sum_{(j,k)\in B} \phi_\lambda(j,k). \tag{6}$$

We assume $n_B$ will remain approximately constant as the boundary evolves. Reworking equation (6), we get:

$$\Phi_\lambda(B) \approx \frac{\gamma}{n_B} \sum_{(j,k)\in B} (\phi_\lambda(j,k) - \frac{\beta n_B}{\gamma}(\lambda_j - \lambda_k)^2)$$

$\Phi_\lambda(B)$ can be minimized using the level set technique. But for this minimization to be meaningful with regard to the length functional defined in equation (3), we define the difference map over the Cartesian coordinate system that is rotated 45° from the coordinate system of the image. (See Figures 1 and 2; every black dot in Figure 2 is a line in Figure 1.) Note that this idea can be easily applied to a 3-D image to form a 3-D difference map.

On the other hand, when $B$ is fixed:

$$\Phi_B(\lambda) = \frac{1}{2}\|y - \mathbf{A}\lambda\|^2_{\mathbf{W}} + \beta R_B(\lambda) + \frac{\gamma}{n} S_B(\lambda) \quad (7)$$

$$S_B(\lambda) = \sum_{(j,k)\in B} \phi_\lambda(j,k). \quad (8)$$

Here we could approximate $\phi_\lambda$ by a quadratic function using Taylor series, but the point around which $\phi_\lambda$ is expanded must be close enough to the actual value. This point could be calculated using data obtained from the previous iteration. We ignore this term in the current implementation. This should have a small effect on the final result; since this term penalizes small differences between pixel values across the boundary, but does not "reward" very large differences; and since the pixel values have been decoupled across the boundary by $R_B(\lambda)$, they will have large differences anyway. Since this objective is quadratic, it is easily minimized using the conjugate gradient method [10].

We also incorporate a deterministic annealing scheme into our minimization, so that the algorithm does not converge to a bad local minimum. (During the annealing procedure, the $h(j,k,B)$'s close to the estimated boundary are evolved toward the function described in equation (4).) We run the alternating minimization scheme, until $\lambda$ and $B$ converge, presumably to a local minima.

## 5 Multiple Regions and Contours

To extend this approach to multiple regions, we first manually determine the number of regions from the initial estimate of the image. The number of regions is assumed to be constant; it is denoted $M$. Then we have a boundary defined for each of these regions. We modify the objective function:

$$\Phi(\lambda, B) = \frac{1}{2}\|y - \mathbf{A}\lambda\|^2_{\mathbf{W}} + \beta R(\lambda, B) + \sum_{i=1}^{M} \frac{\gamma}{n} S_i(\lambda, B_i)$$

$$R(\lambda, B) = \sum_{(j,k)\in N} h(j,k,B)(\lambda_j - \lambda_k)^2$$

$$S_i(\lambda, B_i) = \sum_{(j,k)\in B_i} \phi_\lambda(j,k),$$

where $B_i$ is the $i$th boundary, $B$ is the union of all $B_i$'s. When minimizing with regard to $B$, we initialize the curve either inside or outside a particular region and then perform front propagation using level sets for that region. Similar to the 2-region case, deterministic annealing is also employed. We used the following phantom image to test our method (Figure 3). The reconstructed image and its profile are shown in Figures 4 and 5. Note that there is some error in the boundary extraction due to noise in the sinogram, but the boundary extraction at this noise level is largely accurate.

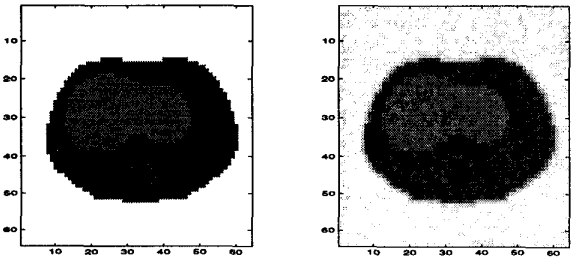

Figure 3: Multiple-region phantom and an FBP reconstruction

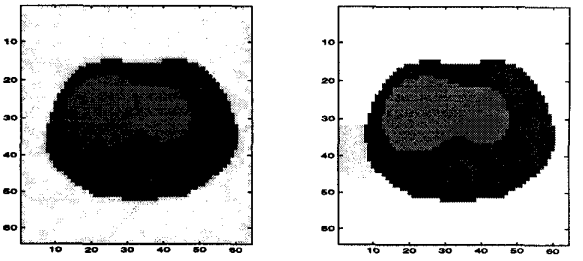

Figure 4: Reconstruction using local Huber penalty and new method

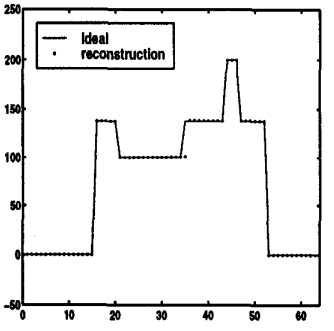


Figure 5: A profile of column 31 of the reconstructed image

## 6 Experimental Results

For simplicity, we performed simulations using equation (1) on a 1-contour image with white Gaussian noise added to the sinogram. $Y$ is a 100 by 100 sinogram, $\lambda$ is a 64 by 64 phantom image consisting of a disk and its background, the pixel values are 200 inside the disk (ROI), and 0 outside. In this preliminary implementation, we ignore $-\frac{\beta n}{\gamma}\sum_{(j,k)\in B}(\lambda_j - \lambda_k)^2$ in $\Phi_\lambda(B)$ when we minimize with regard to $B$ with $\lambda$ fixed, and $\sum_{(j,k)\in B}\phi_\lambda(j,k)$ in $\Phi_B(\lambda)$ when we minimize with regard to $\lambda$ with $B$ fixed. Neither of these terms will have too much effect on the final result. The phantom image and a FBP reconstruction

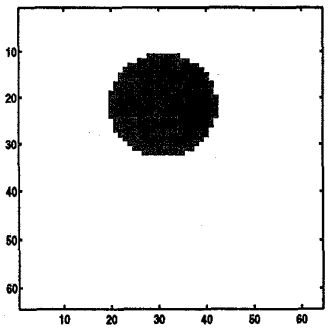

Figure 6: Phantom image

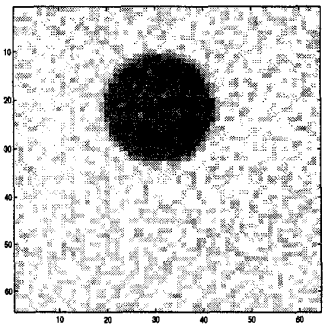

Figure 7: FBP reconstruction

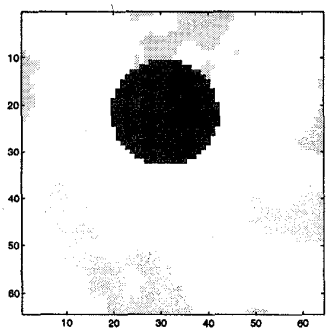

Figure 8: Reconstructed image using proposed algorithm

are shown in Figures 6 and 7. The final reconstruction using the proposed algorithm is shown in figure 8; A reconstruction using the PLS algorithm with nonquadratic local regularization is shown in figure 9; a profile comparison of 2 methods is shown in figure 10. The reconstructed image using local regularization tends to drop off near the edge, while the one using nonlocal regularization remains flat to the edge.

We also did some bias/variance tradeoff studies of the two algorithms. We ran 50 realizations for each algo-

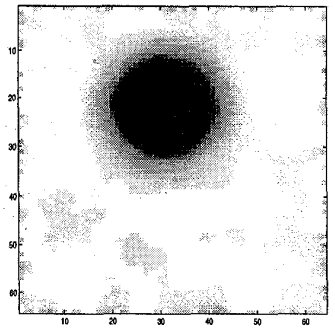

Figure 9: Reconstructed image using PLS algorithm with local nonquadratic penalty

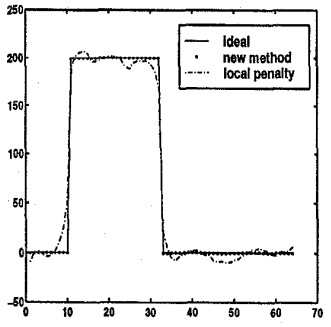


Figure 10: A profile of the reconstructed image

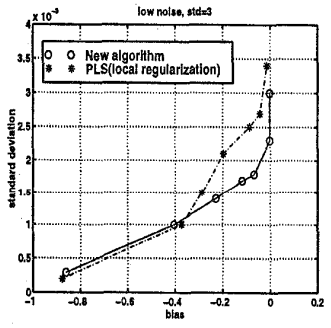


Figure 11: Bias/variance comparison for the low noise case

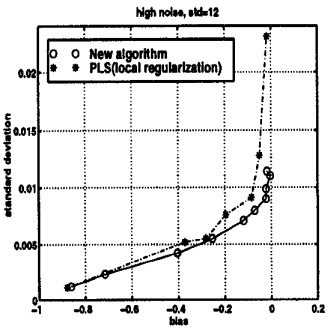


Figure 12: Bias/variance comparison for the high noise case

rithm for two noise levels, one with standard deviation 3 (low noise), and the other with standard deviation 12 (high noise) (the maximum value of the noiseless sinogram is about 48). We then took the average value of the reconstructed image inside the ROI; this gave us 50 numbers for each noise level. We also post-smoothed the image of the lowest variance obtained using the new algorithm. The standard deviation of each group of 50 numbers is plotted against the estimate bias in figures 11 and 12, respectively.

We can see that our new edge-preserving reconstrunction method with global regularization yields lower variance when bias level is below 30% under the low noise case, and lower variance when bias level is below 60% under the high noise case, when compared to conventional local regularization method.

## 7 Conclusion and Future Work

The simulations presented here point out the potential advantage of considering nonlocal boundary information in the regularization. We hope to apply this approach to 3-D data eventually. Information from the 3rd dimension should provide improvement in our regularization, thus achieving lower variance.

## Acknowledgments

This work is supported in part by the Whitaker Foundation and NIH grants CA-60711 and CA-54362.

## References

[1] P. Charbonnier, L. Blanc-Féraud, G. Aubert, and M. Barlaud, "Deterministic edge-preserving regularization in computed imaging," *IEEE Tr. Im. Proc.*, vol. 6, no. 2, , February 1997.

[2] L. Bedini, E. Salerno, and A. Tonazzini, "Edge-preserving tomographic reconstruction from Gaussian data using a Gibbs prior and a generalized expectation-maximization algorithm," *Intl. J. Imaging Sys. and Tech.*, vol. 5, no. 3, pp. 231–8, 1994.

[3] S. Kichenassamy, A. Kumar, P. Olver, A. Tannenbaum, and A. Yezzi, "Conformal curvature flows: from phase transitions to active vision," *Archive for Rational Mechanics and Analysis*, vol. 134, no. 3, pp. 275–301, 1996.

[4] A. Yezzi, S. Kichenassamy, A. Kumar, P. Olver, and A. Tannenbaum, "A geometric snake model for segmentation of medical imagery," *IEEE Tr. Med. Im.*, vol. 16, no. 2, pp. 199–210, April 1997.

[5] S. Teboul, L. Blanc-Feraud, G. Aubert, and M. Barlaud, "Segmentation and edge-preserving restoration," *ICIP 97*, 1997.

[6] J. A. Fessler, "Grouped coordinate descent algorithms for robust edge-preserving image restoration," in *Proc. SPIE 3071, Im. Recon. and Restor. II*, pp. 184–94, 1997.

[7] K. Sauer and C. Bouman, "A local update strategy for iterative reconstruction from projections," *IEEE Tr. Sig. Proc.*, vol. 41, no. 2, pp. 534–548, February 1993.

[8] S. Osher and J. A. Sethian, "Fronts propagation with curvature dependent speed: Algorithms based on Hamilton-Jacobi formulations," *Journal of Computational Physics*, vol. 79, pp. 12–49, 1988.

[9] R. Malladi, J. A. Sethian, and B. C. Vemuri, "Shape modeling with front propagation: a level set approach," *IEEE Tr. Patt. Anal. Mach. Int.*, vol. 17, no. 2, pp. 158–76, February 1995.

[10] W. H. Press, S. A. Teukolsky, W. T. Vetterling, and B. P. Flannery, "Numerical recipes in c,", 1992.